Phosphorus, Sulfur, and Silicon and the Related Elements

ISSN: (Print) (Online) Journal homepage: https://www.tandfonline.com/loi/gpss20

A comparative conformational study of $(C_6H_5O)_2P(O)(NHC(S)NHCH_2C_6H_5)$ and analogous X-ray structures: energy calculations (solid-state/gas phase)

Saeed Hosseinpoor, Mehrdad Pourayoubi, Michal Dušek & Eliška Skořepová

To cite this article: Saeed Hosseinpoor, Mehrdad Pourayoubi, Michal Dušek & Eliška Skořepová (2021): A comparative conformational study of $(C_6H_5O)_2P(O)(NHC(S)NHCH_2C_6H_5)$ and analogous X-ray structures: energy calculations (solid-state/gas phase), Phosphorus, Sulfur, and Silicon and the Related Elements, DOI: 10.1080/10426507.2021.2021523

To link to this article: https://doi.org/10.1080/10426507.2021.2021523

PHOSPHORUS, SULFUR, AND SILICON AND THE RELATED ELEMENTS
https://doi.org/10.1080/10426507.2021.2021523

A comparative conformational study of $(C_6H_5O)_2P(O)(NHC(S)NHCH_2C_6H_5)$ and analogous X-ray structures: energy calculations (solid-state/gas phase)

Saeed Hosseinpoor[a], Mehrdad Pourayoubi[a], Michal Dušek[b], and Eliška Skořepová[b]

[a]Department of Chemistry, Faculty of Science, Ferdowsi University of Mashhad, Mashhad, Iran; [b]Institute of Physics of the Czech Academy of Sciences, Prague 8, Czech Republic

ABSTRACT

The crystal structure of diphenyl (benzylcarbamothioyl)phosphoramide, $(C_6H_5O)_2P(O)(NHC(S)NHCH_2C_6H_5)$, is reported. In the P(O)NHC(S)NH moiety the conformations are *−ap/+ap/−sp*, based on the O = P-N-C/P-N-C-N/P-N-C = S torsion angles (*ap* = antiperiplanar and *sp* = synperiplanar), which are different from the conformations of similar moiety in analogous structures retrieved from the Cambridge Structural Database (CSD). The calculated energies of the most stable seven conformers of the title compound (gas phase) are compared with the conformer found in the crystal structure, and the latter shows a relatively high energy value. In the crystal structure, a double-layered two-dimensional supramolecular assembly, along the *bc* plane, is mediated through (N-H···)(N-H···)O = P and $\pi\cdots\pi$ interactions, with cooperation from C-H···π, C-H···O and C-H···S. Energy framework calculations show the significant role of N-H···O hydrogen bonds in the *c* direction and the weak interactions with mainly dispersion component in the other two directions. The hydrogen bonds and weak interactions were confirmed by the quantum theory of atoms in molecules (AIM).

ARTICLE HISTORY
Received 12 July 2021
Accepted 17 December 2021

KEYWORDS
N-phosphorylated thiourea; conformation; crystal structure; energy calculation; energy framework; hydrogen bond pattern

GRAPHICAL ABSTRACT

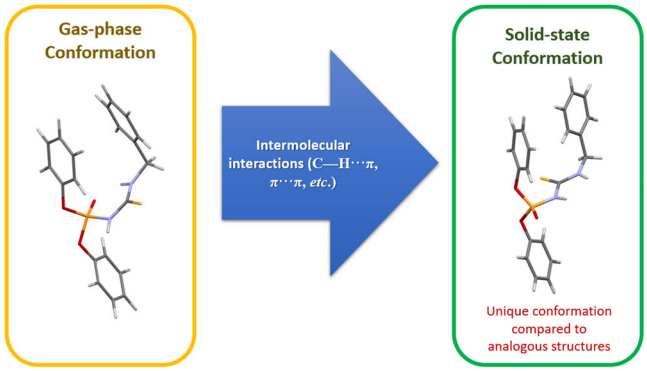

Introduction

Molecular conformation is an influential factor in the molecular surface-dependent properties (including hydrophobicity and some biological activities).[1,2] The electronic nature and energies[3–5] of the conformers and production of conformational polymorphs[6] were investigated. Some studies have been focused on the conformations that molecules choose in the absence of crystal packing force (gas-phase) as well as available conformers in the crystallization solution.[7] The tendency of each conformational isomer to crystallize and the interplay between the experimentally observed conformer and hydrogen bond pattern were studied.[7,8]

Non-covalent intramolecular interactions have an important role in determining the population distribution of conformers and the preferred conformer in the solution phase. Besides, intermolecular interactions in the crystal phase determine the energy level of crystals associated with possible conformers, which can be a comparative indicator of thermodynamical desirability for the crystallization of the possible polymorphs. Therefore, investigating intra/intermolecular interactions can be helpful to make insight into the crystallization process of flexible molecules.

The *N*-phosphorylated thioureas, with the P(O)NHC(S)NH skeleton, have attracted attention due to the diversity of their coordination behavior, such as the possibility of using anionic/neutral forms and coordinating through different donor atoms,

CONTACT Mehrdad Pourayoubi pourayoubi@um.ac.ir Department of Chemistry, Faculty of Science, Ferdowsi University of Mashhad, Mashhad, Iran.
Supplemental data for this article is available online at https://doi.org/10.1080/10426507.2021.2021523.

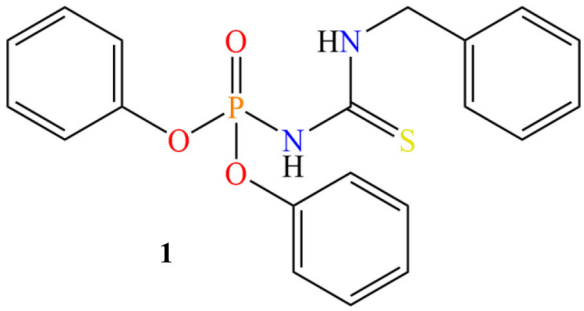

Figure 1. Structure of the phosphorylated thioamide investigated **1**.

and versatility of coordination modes around the central metal cation.[9–12]

In this article, we study the structural/spectroscopic features of a new *N*-phosphorylated thiourea, i.e., $(C_6H_5O)_2P(O)(NHC(S)NHCH_2C_6H_5)$ **1** (Figure 1), and molecular/quantum mechanics calculations are implemented to find different stable conformers (gas-phase). The calculated geometries/energies of conformers in the gas phase are compared with the ones for the conformer observed in the solid state. The crystal lattice energy is calculated, and the energy framework is studied to better perceive molecular packing and intermolecular interactions. The differences/similarities of structural geometry and intermolecular packing of the new structure are compared with the analogous structures retrieved from the Cambridge Structural Database (CSD, version 5.42, updated to Feb 2021),[13] and the factors such as the type of substituent, flexibility, and inter-/intramolecular contacts are considered.

Results and discussion

Spectroscopic study

In the IR spectrum the P = O and NH stretching frequencies appear at the bands centered at 1206 cm^{-1} and 3353/3140 cm^{-1}, respectively. The mass spectrum shows the molecular ion peak (m/z = 398 amu).

The phosphorus signal in $^{31}P\{^1H\}$ NMR spectrum appears at −10.8 ppm as a singlet (Figure S1). In the ^1H NMR spectrum, the doublet at 4.75 ppm ($^3J_{HH}$ = 5.6 Hz) is associated with the protons of CH_2 fragment coupled with vicinal proton (of NH). The two NH protons appear as a triplet at 8.87 ppm ($^3J_{HH}$ = 5.7 Hz) and a singlet at 10.08 ppm (Figure S2). In the $^{13}C\{^1H\}$ NMR spectrum, the doublets at 121.0 ppm (J = 4.7 Hz) and 150.2 ppm (6.5 Hz) are related to the *ortho* and *ipso* carbon atoms of the phenoxy groups and the doublet at 181.7 ppm (3.3 Hz) corresponds to the carbon of the thiocarbonyl group (Figure S3).

X-ray diffraction studies

The title compound, $P(O)(OC_6H_5)_2(NHC(S)NHCH_2C_6H_5)$, crystallizes in the monoclinic space group $P2_1/c$, and the asymmetric unit is composed of one molecule (Figure 2). Selected bond lengths and angles and hydrogen bond geometry parameters are given in Tables 1 and 2. In general, all bond lengths and angles are within the expected values

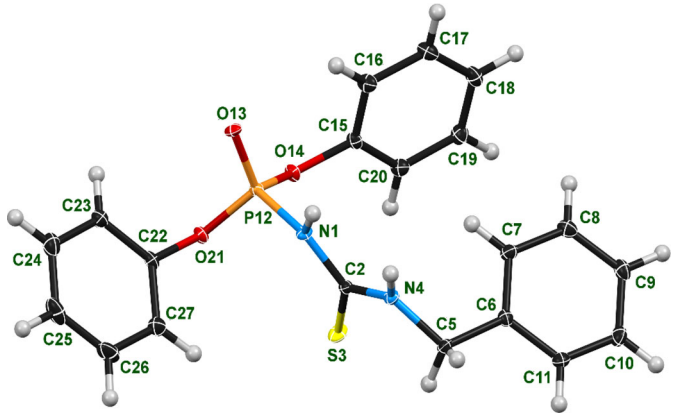

Figure 2. Molecular structure in the crystal of the thioamide **1** and atom-labeling scheme. Displacement ellipsoids are drawn at the 50% probability level.

Table 1. Selected geometric parameters (Å, °) for **1**.

N1-C2	1.393 (2)	P12-O13	1.474 (1)
N1-P12	1.644 (1)	P12-O14	1.573 (1)
C2-S3	1.663 (2)	P12-O21	1.571 (1)
C2-N4	1.341 (2)	O14-C15	1.415 (2)
N4-C5	1.455 (2)	O21-C22	1.424 (2)
C2-N1-P12	128.7 (1)	N1-P12-O21	111.7 (1)
N1-C2-S3	122.8 (1)	O13-P12-O21	115.3 (1)
N1-C2-N4	112.4 (1)	O14-P12-O21	97.1 (1)
S3-C2-N4	124.8 (1)	P12-O14-C15	122.1 (1)
C2-N4-C5	123.9 (1)	O14-C15-C16	121.7 (1)
N4-C5-C6	113.9 (1)	O14-C15-C20	116.0 (1)
N1-P12-O13	106.5 (1)	P12-O21-C22	117.9 (1)
N1-P12-O14	110.1 (1)	O21-C22-C23	119.3 (1)
O13-P12-O14	116.0 (1)	O21-C22-C27	117.7 (1)

according to those observed in analogous structures; for example the P = O bond length is 1.474 (1) Å, and the bond angles at the P atom are between 97.1 (1)° and 116.0 (1)°. The two N atoms adopt a practically planar environment with the bond angle sums of 357.7° and 360°.

The O = P-N-H torsion angle (−7.3°) shows a synperiplanar conformation (−*sp*) of P = O group and its bonded N-H unit, and the two NH units are in an *anti*-position relative to the C = S group (±*ap* conformation, according to the values of 178.6° and −174.7° for the corresponding torsion angles; *ap* = antiperiplanar). The conformations in the P(O)NHC(S)NH fragment were also considered based on the O = P-N-C/P-N-C-N/P-N-C = S torsion angles. These torsion angles are −169.1°/161.3°/−19.5°, showing the −*ap*/+*ap*/−*sp* conformations. As will be discussed in the next section, the conformations in the title structure are different from the other reported analogous structures, especially in the O = P-N-C torsion angle. For a typical example, we consider the structure with refcode SOKDUT, which is the most similar structure to the title compound and which just lacks the CH_2 moiety attached to the arene ring. The different conformations reflect the intramolecular interaction C5-H51···S3 (CH unit belongs to the CH_2 moiety) in the title structure.

The phenyl ring of benzyl moiety (C6-C11) is closer to the C15-C20 ring relative to the other ring (C22-C27) with the distances between their centroids of 5.077 and 9.431 Å.

Table 2. Hydrogen-bond geometry parameters (Å, °) for **1**.

D-H···*A*	*D*-H	H···*A*	*D*···*A*	*D*-H···*A*
C16-H161···O13	0.94	2.58	3.207 (2)	125
N1-H11···O13^{i}	0.85	1.91	2.756 (2)	173 (1)
N4-H41···O13^{i}	0.84	2.43	3.151 (2)	145 (1)

Symmetry code: (i) $x, -y+3/2, z-1/2$.

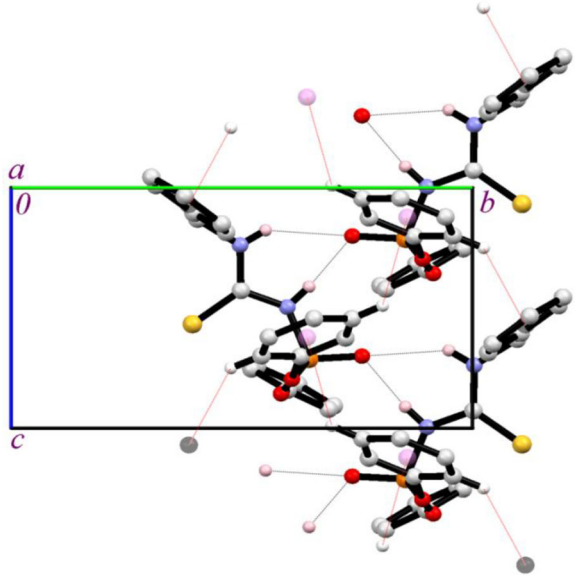

Figure 3. View of one-dimensional array, made by N-H···O = P hydrogen bonds (dotted black lines) and C-H···π interactions (dotted red lines), parallel to the *c* axis. The hydrogen atoms not involved in hydrogen bond interactions have been omitted for clarity. The centroids of phenyl rings are shown as gray and violet balls.

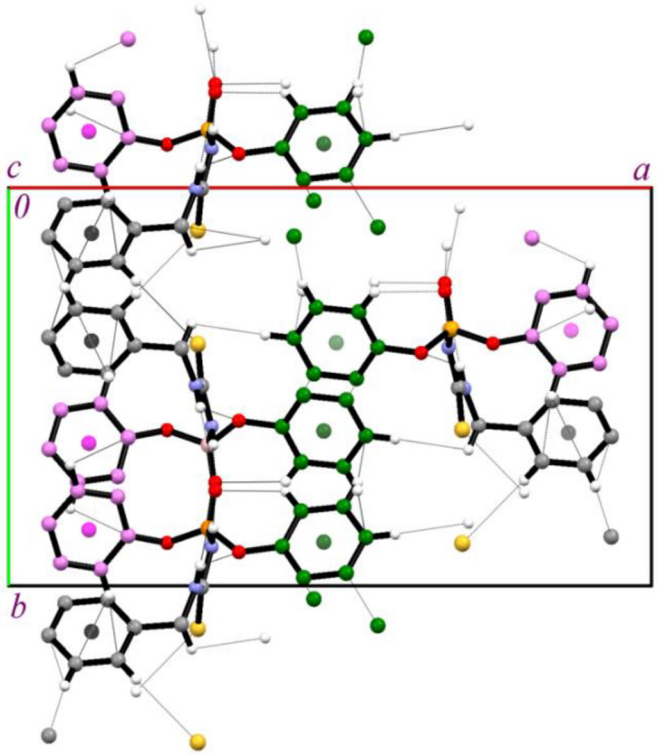

Figure 4. A view of the two-dimensional arrangement (along *bc*) including (N-H)$_2$···O = P, C-H···π, C-H···S, C-H···O, π···π and H···H interactions. The H atoms not involved in the interactions noted were omitted for clarity. The centroids of phenyl rings were shown as green, gray and violet balls.

In the crystal, the molecules are assembled through (N-H)$_2$···O = P hydrogen bonds in a one-dimensional zig-zag array parallel to the *c* axis, including $R_2^1(6)$, $C_1^1(4)$, $C_1^1(6)$, and $C_2^2(10)$ graph-set motifs. The possible C-H···π interactions, between the C20-H201 unit and C6-C11 ring (H···Cg1 = 2.625 Å) and C17-H171 unit and C15-C20 ring (H···Cg2 = 2.788 Å), do not change the dimensionality made by the N-H···O hydrogen bonds (Figure 3).

The presence of two NH units, three arene rings, three oxygen atoms, and one sulfur atom as well as flexibilities in some segments cause the involvement of different sections of molecule in the significant inter-/intra-molecular contacts. Henceforth, for better illustration of different contacts and the connection between these rings, different colors, gray (C6-C11), violet (C15-C20), and green (C22-C27), are used for representation of rings (Figures 4 and 5).

The noted neighboring one-dimensional assemblies are interconnected into slabs (along the *bc* plane) through the possible π···π interaction between the symmetry-related green rings (Cg3···Cg3 = 3.678 Å) (Figure 4). In the two-dimensional assemblies formed, the connections related to the rings (also including the contacts noted so far) are as follows: the violet ring takes part in the C-H···π interactions as both donor and acceptor, in the connection with violet/gray (double-donor) and violet ring, respectively. The gray ring acts as donor, in the C-H···π (acceptor is a gray ring) and C-H···S interactions, and as acceptor (donors are violet and gray rings). The green ring takes part in the C-H···π, C-H···O and π···π. Considering the new introduced contacts the dimensionality is not changed to a three-dimensional arrangement; however, the overall effect of all contacts is the formation of a double-layered 2D array, with a thickness of 18.55 Å (Figure 5). These probable weak contacts are C11-H111···S3 (H···S = 2.947 Å), C23-H231···O13 (H···O = 2.806 Å), C-H···π (C10-H101···Cg3, H···Cg3 = 2.925 Å) and N4-H41···O21 (H···O = 2.678 Å). The intramolecular C5-H51···S3 (H···S = 2.698 Å) and C16-H161···O13 (H···O = 2.58 Å) also exist, which affect the observed conformations including C = S moiety (as discussed earlier) and arene ring. The *para*-H atom of the green ring is near to the H atom of CH_2 moiety (H···H = 2.406 Å).

CSD analysis

Comparison of geometrical data

In this section, the phosphorylated thiourea structures, with the general formula $(R^1O)_2P(O)NHC(S)NHR^2$ (Table S1), available in the CSD are studied and compared with the structure of **1**. The dataset includes 11 structures,[14–23] the cif file of one of which is not available. The P = O and P-N bond lengths were compared and the results were gathered in Table S2. These bond lengths are between 1.459–1.482 Å and 1.640–1.679 Å, respectively. In all structures, the bond-angle sums at the two N atoms are near to (or equal with) 360°, which show planar environments around the N atoms. The geometrical data of the title structure fit well with the CSD structures. Typically, the P-N bond length of the title

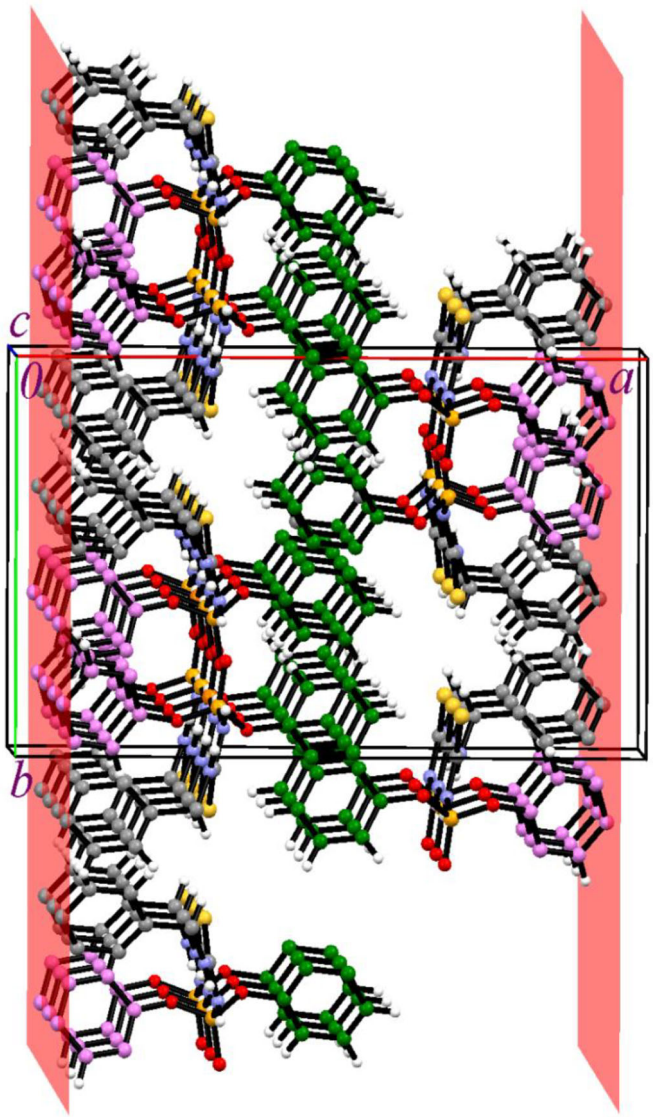

Figure 5. A view of a double-layered two-dimensional array of the title structure, the thickness is 18.55 Å, based on the spatial distance between mean planes shown. The mean planes were generated considering the boundary carbon atoms.

structure is 1.644 (1) Å, which shows about 30% π character along with the phosphorus-nitrogen σ bond.[24]

Conformations of P(O)NHC(S)NH segments

The conformational analysis was performed on the P(O)NHC(S)NH segment of the $(R^1O)_2P(O)NHC(S)NHR^2$ structures, and the influence of substituents attached to this segment and the relationship with the hydrogen bond pattern were considered, as illustrated in Figure 6. The conformational analysis was done based on the O = P-N-C/P-N-C-N/P-N-C = S torsion angles.

In the P(O)NHC(S)NH segment, oxygen and sulfur are two electron-rich atoms capable of hydrogen bonding interactions, however, the hydrogen bond acceptor capabilities are quite different. Out of the 11 structures investigated, only two structures show NH···S = C hydrogen bonds, but all of the structures include NH···O = P hydrogen bonds. Furthermore, the ester oxygen atoms (P-O-C) do not cooperate in significant hydrogen bond interactions, showing their low Lewis base characteristics.

The structures SOKDUT and RUYHAW include R^1 = C_6H_5 and R^2 = C_6H_5 and 3-ClC_6H_4, respectively. Both these structures show ±*sc*/±*ap*/±*sp* conformations (*sc* = synclinal), two intermolecular NH···O = P hydrogen bonds, and no intramolecular hydrogen bonding. The structure with refcode OFESEZ and the title structure also include R^1 = C_6H_5, however, R^2 is not a phenyl derivative, with the conformations of +*sp*, −*sc*/±*sp*/±*ap* and −*ap*/+*ap*/−*sp*, respectively. The type of hydrogen bonds in the title structure is similar to the ones in SOKDUT and RUYHAW, but probably the main difference in the torsion angles is related to the near intramolecular CH···S = C contact in the title structure (the CH belongs to the flexible benzyl group) which changes all of the three torsion angles investigated. Typically, the different O = P-N-C torsion angles, −169.13° (**1**) and 53.78° (SOKDUT) reflect different conformations.

The orientation of the P = O group relative to the C = S group in **1**/OFESEZ is different from the one with SOKDUT/RUYHAW, *i.e.,* these groups have the opposite directions in the first pair and a similar direction in the second pair.

The conformation of MURDUZ is −*sc*/−*ap*/+*sp* (−66.92°/−168.24°/10.56°) and the effect of pyridine ring and the existence of intramolecular N-H···N hydrogen bond is mainly seen in the O = P-N-C torsion angles in comparison with the structures SOKDUT/RUYHAW, but the variations are too little to change the conformations (apart from the sign).

The other compounds are AQINOE, GODNIX, HUMJUV, UGOHUU, ROZXOU, and ROZXIO (at least R^1 or R^2 ≠ phenyl derivatives). These compounds adopt the ±*sc*, ±*sp*/±*sp*/±*ap* conformations, and the intramolecular NH···O = P hydrogen bonding is observed in all of them (Figure 6). This interaction is responsible for the internal twisting of the amine moiety and as a result the thiocarbonyl group. The conformations in these structures are almost like the one observed for OFESEZ, and the torsion angles show a similar situation for the P-N-C(S)-N segment, while the flexibility is seen in the P(O) group relative to the residual segment.

The calculated energies of possible conformers of the title compound

To compare the conformer observed in the solid-state with the ones expected in the absence of crystal packing interactions (gas phase), firstly, the most stable conformers were searched by *Spartan 14*[25] using the Merck Molecular Force Field (MMFF) method. For 100 conformers obtained, firstly, equilibrium geometry calculations in vacuum were performed using the semi-empirical PM6 method. Then for the 30 more stable conformers, similar calculations were implemented using the HF/3-21G *ab initio* method. 23 structures with Boltzmann's distribution by less than 1% were

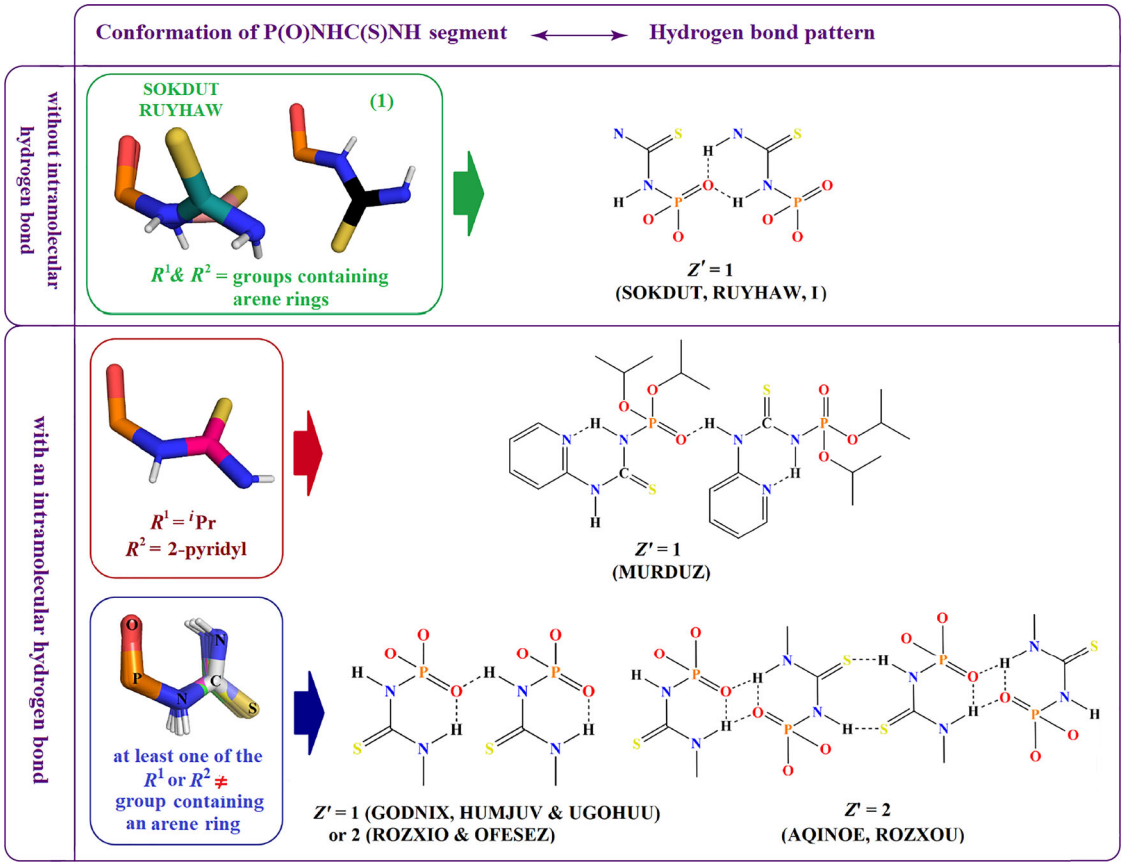

Figure 6. Interplay of conformations of P(O)NHC(S)NH segment and hydrogen bond patterns in the reported $(R^1O)_2P(O)(NHC(S)NHR^2)$ structures. The overlay has been shown for the P(O)NHC(S)NH segment and some of the groups in figures of hydrogen bond patterns have not been drawn.

excluded. The remaining 7 conformers and the title structure **1** were optimized by the M06-2X/6-311++G(d,p) method using the *Gaussian09* software.[26] The structures of the conformers and the energy differences of these conformers relative to the most stable one are shown in Figure 7.

The results show that the difference between the energy of **1** and the most stable conformer (IA) is about 25 kJ/mol, and in the absence of intermolecular interactions, the conformation in solid state of **1** is not preferred in the gas phase. It seems that in the crystal structure, the extensive contacts force the studied compound into the observed conformation. As can be seen in Figure 7, all of the more stable conformers possess an intramolecular NH···O = P hydrogen bond and adopt a structure similar to most of the other structures retrieved from the CSD (see Figure 6, third row).

Hirshfeld surface analysis and enrichment ratio

To investigate the intermolecular interactions in more detail, the 3D Hirshfeld surface maps[27] and 2D fingerprint plots[28] were generated using *CrystalExplorer 17.5*[29] and the results are shown in Figures 8 and S4, respectively.

In the Hirshfeld surface maps, the red spots (labels 1 and 2) correspond to two intermolecular N-H···O = P hydrogen bonds and pale red spots (labels 3 and 4) are related to H251···H51 and C20-H201···C11 interactions. The 2D fingerprint plots manifest the highest contribution of H···H (47.4%) and then C···H (26%) and O···H (13.8%) contacts relative to the total contacts in the crystal. For O···H, intermolecular hydrogen bonds develop two distinct spikes, and for C···H, two wings show the C-H···π interactions. The S···H (7.4%) and C···C contacts (3.2%) are also significant, and the other contacts have negligible contributions, with the sum of their percentages less than 3%.

The enrichment ratios (E_{xy}) of the title compound were determined using the method reported by Jelsh et al. (2014), by dividing the Hirshfeld surface contact proportion (C_{xy}) to the random contact proportion (R_{xy}). The enrichment ratio is the ratio between the actual contacts proportion in the crystal and theoretical contacts proportion. If this value exceeds unity, the pairs of elements have a high propensity to form contacts, and if it is less than unity the pairs of elements avoid contact with each other. The calculated C_{xy}, R_{xy}, and E_{xy} values are given in Table 3. In the table, E_{xy} values for "random contacts" < 1% were not reported, because they are not meaningful.[30]

According to the obtained values, the most favorable contacts are established between the sulfur and hydrogen atoms with E_{xy} equals to 1.396, which shows the desirability of S···H interactions, as shown by Potrzebowski *et al.* for C-H···S contacts.[31] The other favorable contacts are O···H, C···C, and C···H, due to the hydrogen bonds, π···π, and C-H···π interactions, respectively. The E_{xy} value for the C···O

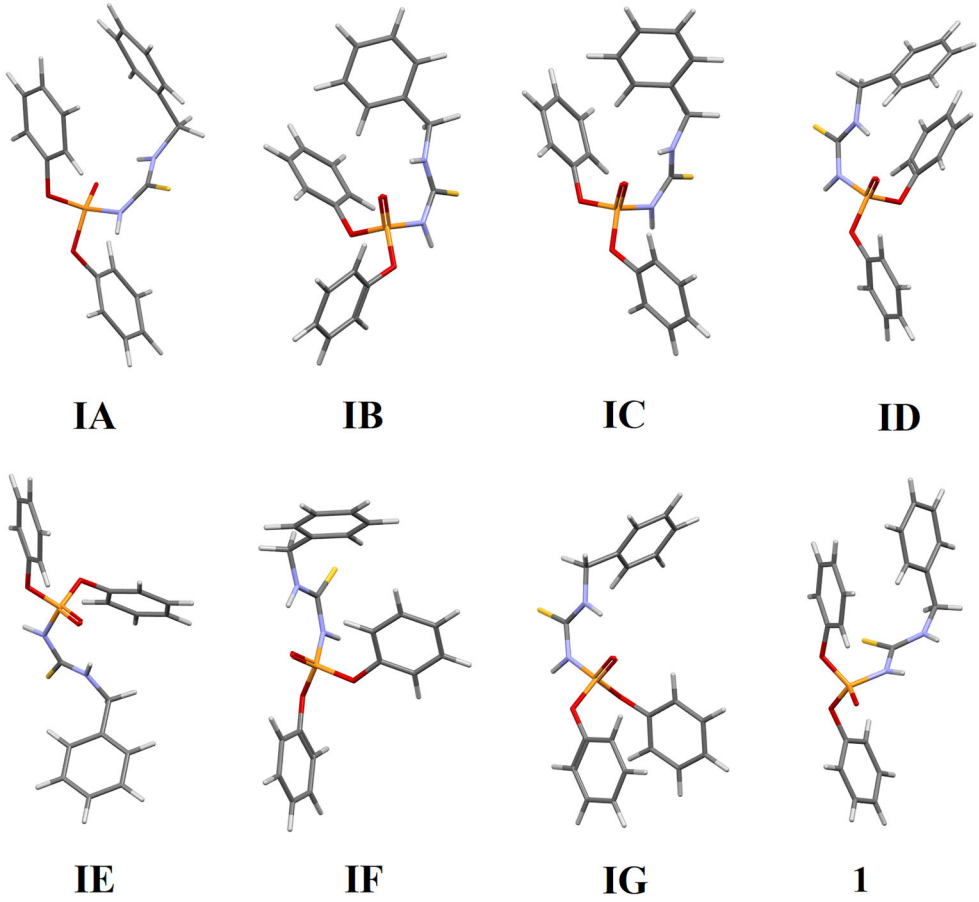

	IA	IB	IC	ID	IE	IF	IG	1
ΔE_{M062X} (kJ/mol)	0	1	3	5	11	11	14	25

Figure 7. Structures of the most stable conformers (IA-IG) in comparison to **1** (experimental, crystal structure). The energy differences are given with respect to the most stable one (IA) (calculated by M062X/6-311++G (d, p)) and the conformers are sorted by their energies.

contacts are smaller than 1, which indicates the low propensity of these interactions to be formed.

Lattice energy and energy framework

To create a comprehensive picture of the interactions in the crystal structure, the crystal lattice energy was calculated with *CrystalExplorer 17.5* software, using CE-B3LYP/6-31G(d,p) electron-density functions.[32,33] The calculated electrostatic, polarization, dispersion, and repulsion energies in the crystal packing were listed in Table 4. The electrostatic, dispersion and total energy frameworks were drawn as red, green, and blue cylinders, respectively (Figure 9).

The sum of electrostatic, polarization, dispersion, and repulsion interactions energies (Σ *N.E*) are equal to −248.6, −70.8, −433.9, and +427.0 kJ/mol, respectively, and the sum of the total energies is −429.1 kJ/mol. The energy framework was discussed for the four pairs with the highest total energies ($E_{tot} < -20$ kJ/mol), which are given as the pairs shown with labels 1, 2, 3 and 4 and suffixes A and B for energy components in Figure 9.

According to the energy frameworks (Figure 9), the electrostatic interactions energies are mostly concentrated along the *c*-axis, which are associated with the middle part of the molecule, *i.e.,* $[(O)_2P(O)NHC(S)NH]$ moiety (Figure 9a), due to the existence of both regions of negative and positive charges in the electrostatic potential map (Figure S5). The biggest contribution of electrostatic interactions (−75.5 kJ/mol) is between the hydrogen-bonded pair of molecules (Pair 1, label 1A in Figure 9). The same two molecules take part in the C-H···π interactions and also involve the highest value of dispersion energy (−70.6 kJ/mol, label 1B) (Figure 9b). The other notable electrostatic interactions with the energy of −26.9 kJ/mol are between the pair of molecules, where the hydrogens of the amine group (N4-H41) and oxygens of the phenoxy groups are present (Pair 2, label 2A in Figure 9). Dispersion energy between these molecules is also high (−44.4 kJ/mol, label 2B), which can be related to the C-H···π interaction between H201 and C6-C11 ring, and some weak intermolecular contacts.

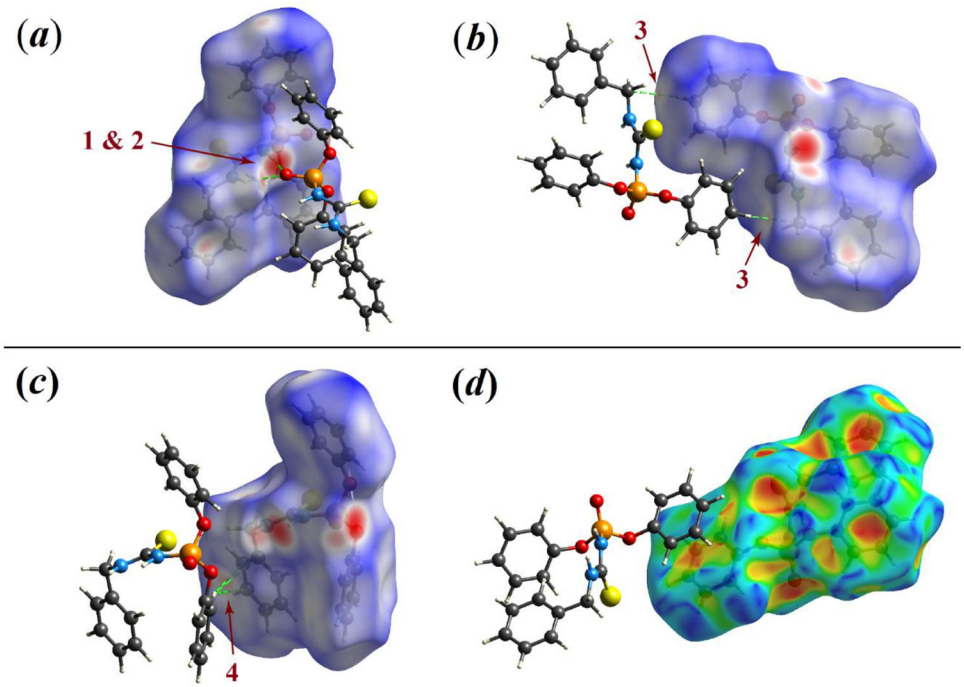

Figure 8. Four views of the Hirshfeld surface of **1** in the vicinity of neighboring hydrogen-bonded/contacted molecules showing (*a*) N-H···O = P hydrogen bonds, (*b*) H···H, (*c*) C-H···π, and (*d*) π···π interactions.

Table 3. "Hirshfeld surface contacts (C_{xy})", "random contacts (R_{xy})" and enrichment ratios (E_{xy}) for the contacts in the structure of **1**.

Contact	C_{xy}	R_{xy}	E_{xy}
H···H	0.474	0.513	0.924
S···H	0.074	0.053	1.396
O···H	0.138	0.110	1.254
C···H	0.259	0.233	1.112
C···C	0.032	0.026	1.231
C···O	0.002	0.025	0.080

Table 4. Calculated interaction energies of the molecular pairs (kJ/mole).

N	Symmetry operation	*R*	E_{ele}	E_{pol}	E_{dis}	E_{rep}	[a]E_{tot}
1	−*x*, −*y*, −*z*	13.25	−1.4	−0.3	−12.6	5.4	−9.4
2	−*x*, *y* + 1/2, −*z* + 1/2	13.32	−1.9	−0.4	−10.2	7.4	−6.6
1	−*x*, −*y*, −*z*	11.29	−2.6	−0.8	−22.3	10.3	−16.4
2	−*x*, −*y* + 1/2, *z* + 1/2	8.31	−8.0	−2.6	−28.9	27.4	−18.6
2	*x*, *y*, *z*	7.08	−26.9	−6.8	−44.4	33.6	−51.3
2	*x*, −*y* + 1/2, *z* + 1/2	6.21	−75.5	−22.4	−70.6	109.7	−90.1
1	−*x*, −*y*, −*z*	9.67	−8.8	−1.9	−44.2	33.4	−28.5
2	−*x*, *y* + 1/2, −*z* + 1/2	11.71	−3.4	−0.9	−8.6	1.9	−10.6
1	−*x*, −*y*, −*z*	11.36	−4.4	−1.6	−29.4	17.9	−20.4
		Σ*N.E*	−248.6	−70.8	−433.9	427.0	−429.1

[a]The scale factors of the electrostatic, polarization, dispersion, and repulsion interactions are equal to 1.057, 0.740, 0.871, and 0.618, respectively.

Dispersion interactions have a dominant role in the *a* and *b* directions, and the more pronounced values are related to the weak hydrogen bonds (Pair 3, label 3B in Figure 9) (−44.2 kJ/mol), and the π···π interaction between the two stacked phenoxy groups (−29.4 kJ/mol) (Pair 4, label 4B in Figure 9).

Accordingly, total energy frameworks (Figure 9c) show that the interactions along the hydrogen bonds are the strongest interactions in the crystal lattice, which are equal to −90.1 and −51.3 kJ/mol, and are responsible for the formation of needle-shaped crystals.

QTAIM analysis

The interactions associated to the pairs 1–4 (see the previous section) were confirmed by quantum theory of atoms in molecules (QTAIM) calculations.[34] For this aim, wfn files were obtained by Gaussian 09 software at the B3LYP-D2/6-311G(d,p) level of theory and QTAIM analyses were performed by the MultiWFN program package.[35] The molecular representations of the bond paths and bond critical points (BCPs) in the studied molecular pairs are shown in Figure 10, wherein the considered interactions are labeled with HB (hydrogen bonds), ΠΠ (π ···π), and HΠ (CH···π). Calculated topological parameters include potential energy density ($V(r)$), kinetic energy density ($G(r)$), total electronic density ($\rho(r)$), and its corresponding Laplacian ($\nabla^2\rho(r)$) at the BCPs (Table 5). The strengths of the hydrogen bonds were estimated by Espinosa and coworkers equation[36] and are given in Table 5. In this method, the strengths of hydrogen bonds are considered equal to half of the potential energy density (E = 0.5 $V(r)$).

The estimated energies for the two significant intermolecular hydrogen bonds, N-H···O = P, and one intramolecular C-H···O = P hydrogen bond are −30.1933 kJ/mol/−7.0888 and −7.8574 kJ/mol, respectively (with ρ(r) = 0.0266/0.0084 and 0.0095 e/Å^3). The most significant CH···π interaction, discussed in the X-ray crystallography section, *i.e.*, H···Cg1, and the π···π interaction, Cg3···Cg3, have the ρ(r) values of 0.0079 and 0.0053 e/Å^3, respectively. Typical examples of some weak contacts are N4-H41···O14 (ρ(r) = 0.0032 e/Å^3), and C25-H251···N4 (ρ(r) = 0.0060 e/Å^3), which are observed in pairs 2 and 3 discussed in the previous section.

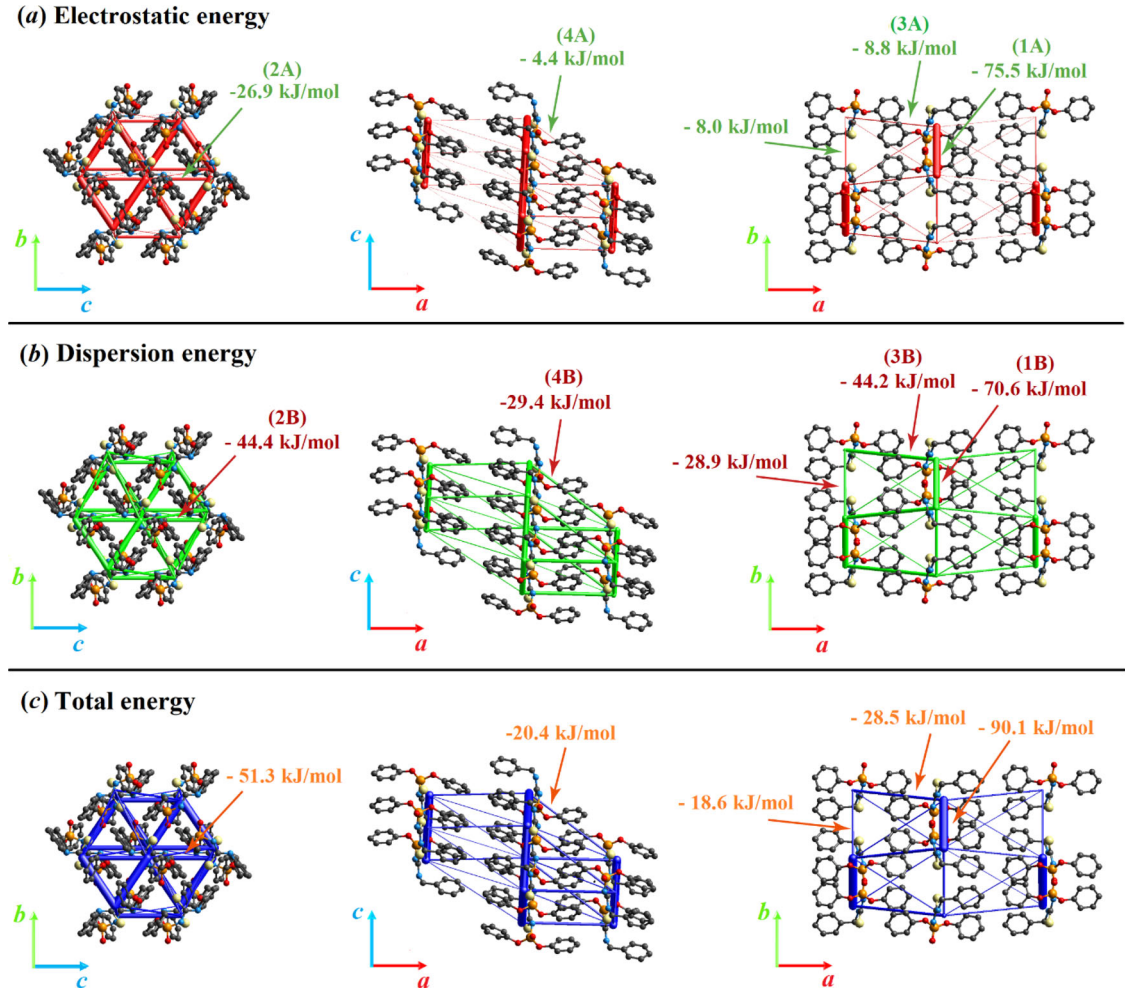

Figure 9. Electrostatic, dispersion, and total energy frameworks and selected energy values for the molecular structure viewed along the *a*, *b*, and *c* directions. Hydrogen atoms have been omitted for clarity.

Conclusion

In the structure of $(C_6H_5O)_2P(O)(NHC(S)NHCH_2C_6H_5)$ the P(O)NHC(S)NH moiety shows the *−ap/+ap/−sp* conformation, which is different from the conformations in analogous structures retrieved from the CSD. The energy frameworks analysis reveals high electrostatic and dispersion attraction energies along the direction of hydrogen bond, and prevailing dispersion interactions in the two other directions. The strongest contribution of interaction energies in the same direction of hydrogen bonds (in one dimension) may be responsible for the formation of needle-shaped crystals. The conformer observed in the solid-state was geometrically/energetically compared with the ones expected in the gas phase, and the amount of force driven by the crystal packing was evaluated. Knowledge about conformational forms of such flexible structures can help to design potential ligands with chelating and/or bridging behavior, that are influenced by the direction of donor groups (P = O/C = S as well as N in an anionic form).

Experimental

Instruments

IR spectrum was recorded with a Buck 500 scientific spectrometer using a KBr disk. The mass spectrum was obtained with a Varian Mat CH-7 instrument at 70 eV. ^{1}H, ^{13}C{^{1}H} and ^{31}P{^{1}H} NMR spectra were recorded with a Bruker Avance DRS spectrometer with frequencies 300.81 MHz, 75.65 MHz, and 121.76 MHz, respectively. Chemical shifts are given relative to TMS for ^{1}H and ^{13}C, and 85% H_3PO_4 for ^{31}P as external standards. The melting point was recorded with an Electrothermal IA 9000 apparatus. X-ray data collection was obtained at 95 K with a single crystal diffractometer SuperNova using mirrors-collimated Cu-Kα radiation ($\lambda = 1.5418$ Å). In the solution and refinement of the structure all H atoms were located in difference maps, but those attached to C atoms were repositioned geometrically. The H atoms were initially refined with soft restraints on the bond lengths and angles to regularize their geometry (C-H in the range 0.93–0.98 Å and N-H in the range 0.86–0.89 Å) and U_{iso}(H) values in the range 1.2–1.5 times U_{eq} of the parent atom, after which the positions were refined with riding constraints.[37] The crystallographic data and details structure refinement are given in Table 6.

Synthesis

A solution of diphenyl phosphoryl chloride (0.814 g, 3.03 mmol) in anhydrous acetonitrile (15 mL) was treated

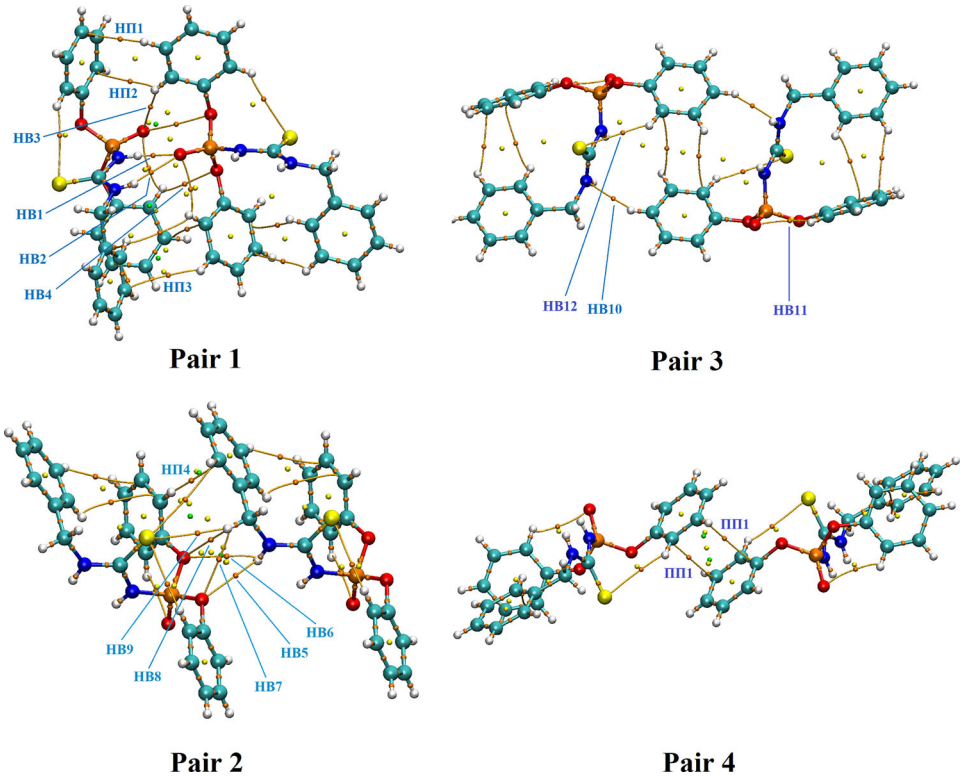

Figure 10. QTAIM plots of the structure I, for the four pairs of molecules with the highest total energies (atom color codes: P = orange, O = red, N = blue, C = cyan, S = yellow, H = white). The more important interactions are labeled with HB (hydrogen bonds), HП (C-H···π), and ППП ($\pi\cdots\pi$).

Table 5. Topological parameters (in atomic unit) and estimated energies (E_{ESP}, kJ/mol) of contacts.

Contacts	Interacting atoms	$\rho(r)$	$\nabla^2\rho(r)$	$V(r)$	$G(r)$	E_{ESP}
HB1	N1-H11···O13	0.0266	0.1207	−0.0230	0.0265	−30.1933
HB2	N4-H41···O13	0.0084	0.0349	−0.0054	0.0071	−7.0888
HB3	C23-H231···O13	0.0051	0.0171	−0.0029	0.0036	−3.8070
HB4	C16-H161···O14	0.0036	0.0147	−0.0022	0.0030	−2.8880
HB5	N4-H41···O21	0.0056	0.0217	−0.0036	0.0045	−4.7259
HB6	N4-H41···O14	0.0032	0.0143	−0.0021	0.0028	−2.7568
HB7	C5-H52···O21	0.0039	0.0157	−0.0025	0.0032	−3.2819
HB8	C5-H52···O14	0.0036	0.0153	−0.0023	0.0031	−3.0193
HB9	C5-H52···S3	0.0045	0.0131	−0.0019	0.0026	−2.4942
HB10	C25-H251···N4	0.0060	0.0196	−0.0035	0.0042	−4.5946
HB11	C16-H161···O13	0.0095	0.0348	−0.0060	0.0073	−7.8574
HB12	C27-H271···S3	0.0046	0.0136	−0.0020	0.0027	−2.6255
CH···π						
HП1	C23-H231···C25	0.0048	0.0132	−0.0022	0.0027	−2.8200
HП2	C23-H231···C23	0.0031	0.0094	−0.0014	0.0019	−1.9007
HП3	C17-H171···C8	0.0028	0.0083	−0.0012	0.0017	−1.6207
HП4	C20-H201···C11	0.0079	0.0241	−0.0038	0.0049	−4.9554
HП5	C7-H71···C15	0.0038	0.0116	−0.0018	0.0023	−2.2536
HП6	C8-H81···C18	0.0047	0.0138	−0.0021	0.0028	−2.7569
$\pi\cdots\pi$						
ППП1	C22···C26	0.0053	0.0139	−0.0023	0.0029	−2.9818

Table 6. Experimental details.

Empirical formula	$C_{20}H_{19}N_2O_3PS$
Formula weight	398.42
Temperature (K)	95
Wavelength (Å)	1.5418
Crystal system	Monoclinic
Space group	$P2_1/c$
a (Å)	20.7959 (2)
b (Å)	12.6194 (1)
c (Å)	7.0779 (1)
α (°)	90
β (°)	93.2084 (8)
γ (°)	90
V (Å^3)	1854.55 (3)
Z	4
D_{calc} (g/cm^3)	1.427
Absorption coefficient (mm^{-1})	2.57
$F(000)$	832
Crystal size (mm)	0.96 × 0.05 × 0.03
θ Range for data collection (°)	4.099–74.892
Index range	$-25 \le h \le 25$ $-15 \le k \le 15$ $-8 \le l \le 8$
Reflections collected	27443
Independent reflections	3781 [R_{int} = 0.114]
Absorption correction	Multi-scan *CrysAlis PRO*[38]
Max and min transmission	0.36 and 0.92
Refinement method	Full-matrix least-squares on F^2
Data/restraints/parameters	3781/8/253
Goodness-of-fit on F^2	0.9858
Final R indices [$I > 2.0\sigma(I)$]	R_1 = 0.0357, wR_2 = 0.0951
R indices (all data)	R_1 = 0.0374, wR_2 = 0.0970
Largest difference in peak and hole (e Å^{-3})	0.39, −0.59

under vigorous stirring with potassium thiocyanate (0.294 g, 3.03 mmol) for 3 hours. The potassium chloride salt was filtered off and the filtrate was allowed to react with benzylamine (0.325 g, 3.03 mmol). After a few minutes, a white and bulky precipitate was obtained. The reaction continued overnight, and then the precipitate (0.847 g) was separated by filtration. The remaining solution was left for slow evaporation at room temperature to yield colorless needlelike crystals, suitable for X-ray diffraction studies, which were separated, washed with acetonitrile, and dried. m.p.: 142 °C. IR (KBr disk, ν, cm^{-1}): 3353, 3140, 3070, 3006, 2948, 1592, 1524, 1492, 1457, 1329, 1272, 1206, 1184, 976, 903, 773, 735, 687. MS (70 eV, EI): m/z (%) = 398 (10) $[M]^+$, 397 (21) $[M-1]^+$, 396 (20) $[M-2]^+$, 212 (14) $[M-2OC_6H_5]^+$, 140

(7) $[P(O)(OC_6H_5)]^+$, 106 (94) $[NHCH_2C_6H_5]^+$, 93 (49) $[OC_6H_5]^+$, 91 (94) $[CH_2C_6H_5]^+$, 77 (95) $[C_6H_5]^+$, 29 (100) $[NHCH_2]^+$. $^{31}P\{^1H\}$ NMR (DMSO-d_6, 121.76 MHz, 297.4 K): $\delta = -10.8$ (*s*). ^1H NMR (DMSO-d_6, 300.81 MHz, 297.4 K): $\delta = 10.08$ (*s*, 1H), 8.87 (*t*, $^3J_{HH} = 5.7$ Hz, 1H), 7.55–7.16 (*m*, 15H), 4.75 (*d*, $^3J_{HH} = 5.6$ Hz, 2H). $^{13}C\{^1H\}$ NMR (DMSO-d_6, 75.65 MHz, 297.9 K): $\delta = 181.7$ (*d*, $^2J_{PC} = 3.3$ Hz), 150.2 (*d*, $^2J_{PC} = 6.5$ Hz), 138.1 (*s*), 130.5 (*s*), 128.9 (*s*), 127.7 (*s*), 127.6 (*s*), 126.2 (*s*), 121.0 (*d*, $^3J_{PC} = 4.7$ Hz), 48.1 (*s*). The Supplemental Materials contains sample ^1H, ^{13}C and ^{31}P NMR spectra of the product (Figures S1–S3).

Acknowledgments

The partial support of this work by Ferdowsi University of Mashhad (research project 3/49072) is gratefully acknowledged. The authors appreciatively acknowledge the Cambridge Crystallographic Data Centre for access to the CSD Enterprise suite. The crystallographic experiment used infrastructure supported by Operational Programme Research, Development and Education financed by European Structural and Investment Funds and the Czech Ministry of Education, Youth and Sports (Project No. SOLID21 CZ.02.1.01/0.0/0.0/16_019/0000760).

Disclosure statement

The authors state no potential conflict of interests.

Supplementary material

CCDC number 2120531 contains the supplementary crystallographic data for this paper. These data can be obtained free of charge from the Cambridge Crystallographic Data Centre via: http://www.ccdc.cam.ac.uk/data-request/cif.

ORCID

Saeed Hosseinpoor http://orcid.org/0000-0002-8141-7996
Mehrdad Pourayoubi http://orcid.org/0000-0001-5608-2111

References

[1] Mezzenga, R.; Mitsi, M. The Molecular Dance of Fibronectin: Conformational Flexibility Leads to Functional Versatility. *Biomacromolecules* **2019**, *20*, 55–72. DOI: 10.1021/acs.biomac.8b01258.

[2] Gras, S. L.; Mahmud, T.; Rosengarten, G.; Mitchell, A.; Kalantar-Zadeh, K. Intelligent Control of Surface Hydrophobicity. *ChemPhysChem.* **2007**, *8*, 2036–2050. DOI: 10.1002/cphc.200700222.

[3] Mondal, P.; Rath, S. P. Cyclic Metalloporphyrin Dimers: Conformational Flexibility, Applications and Future Prospects. *Coord. Chem. Rev.* **2020**, *405*, 213117. DOI: 10.1016/j.ccr.2019.213117.

[4] Hasija, A.; Chopra, D. Exploring Concomitant/Conformational Dimorphism in a Difluoro-Substituted Phosphoramidate Derivative. *Acta Crystallogr. C. Struct. Chem.* **2019**, *75*, 451–461. DOI: 10.1107/S2053229619003589.

[5] Alvarez, M. A.; Saavedra, E. J.; Olivella, M. S.; Suvire, F. D.; Zamora, M. A.; Enriz, R. D. Theoretical Study of the Conformational Energy Hypersurface of Cyclotrisarcosyl. *Cent. Eur. J. Chem.* **2012**, *10*, 248–255. DOI: 10.2478/s11532-011-0136-1.

[6] Cruz-Cabeza, A. J.; Bernstein, J. Conformational Polymorphism. *Chem. Rev.* **2014**, *114*, 2170–2191. DOI: 10.1021/cr400249d.

[7] Yu, L.; Reutzel-Edens, S. M.; Mitchell, C. A. Crystallization and Polymorphism of Conformationally Flexible Molecules: Problems, Patterns, and Strategies. *Org. Process Res. Dev.* **2000**, *4*, 396–402. DOI: 10.1021/op000028v.

[8] Wanat, M.; Malinska, M.; Kutner, A.; Wozniak, K. Effect of Vitamin D Conformation on Interactions and Packing in the Crystal Lattice. *Cryst. Growth Des.* **2018**, *18*, 3385–3396. DOI: 10.1021/acs.cgd.8b00091.

[9] Sokolov, F. D.; Baranov, S. V.; Safin, D. A.; Hahn, F. E.; Kubiak, M.; Pape, T.; Babashkina, M. G.; Zabirov, N. G.; Galezowska, J.; Kozlowski, H.; Cherkasov, R. A. The Influence of the Intramolecular Hydrogen Bond on the 1,3-N,S- and 1,5-O,S-Coordination of N-Phosphoryl-N′-(R)-Thioureas with Ni(II) and Pd(II). *New J. Chem.* **2007**, *31*, 1661–1667. DOI: 10.1039/b702896b.

[10] Safin, D. A.; Sokolov, F. D.; Szyrwiel, Ł.; Baranov, S. V.; Babashkina, M. G.; Gimadiev, T. R.; Kozlowski, H. Monodentate S-vs. Bidentate 1,5-O,S-Coordination of N-Phosphoryl-N′-(R)-Thioureas with Pd(II). *Polyhedron* **2008**, *27*, 1995–1998. DOI: 10.1016/j.poly.2008.03.012.

[11] Safin, D. A.; Babashkina, M. G.; Klein, A.; Nöth, H.; Bolte, M.; Krivolapov, D. B. Solvent-Dependent Formation of Two Different Cd(II) Complexes with *p*-$BrC_6H_4C(S)NHP(O)(OiPr)_2$ (HL). Crystallographic Modification of $Cd(HL)_2L_2$. *Polyhedron* **2010**, *29*, 1837–1841. DOI: 10.1016/j.poly.2010.02.031.

[12] Safin, D. A.; Babashkina, M. G.; Bolte, M.; Szyrwiel, Ł.; Klein, A.; Kozlowski, H. Complexes of Co(II) and Zn(II) with *N*-(Thio)Phosphorylthioureas $AdNHC(S)NHP(O)(OiPr)_2$ and $MeNHC(S)NHP(S)(OiPr)_2$. *Phosphorus Sulfur Silicon Relat. Elem.* **2010**, *185*, 1739–1745. DOI: 10.1080/10426500903251365.

[13] Groom, C. R.; Bruno, I. J.; Lightfoot, M. P.; Ward, S. C. The Cambridge Structural Database. *Acta Crystallogr. B. Struct. Sci. Cryst. Eng. Mater.* **2016**, *72*, 171–179. DOI: 10.1107/S2052520616003954.

[14] Osipova, O. V.; Terekhova, M. I.; Bizyaeva, A. Y.; Kolesova, V. A.; Petrov, E. S.; Bel'skii, V. K. Equilibrium NH Acidity of 4-Phosphorylated Allophonates and Thioallophonates. *Zh. Obshch. Khim.* **1989**, *59*, 616–621.

[15] Babashkina, M. G.; Robeyns, K.; Filinchuk, Y.; Safin, D. A. Detailed Studies of the Interaction of 3-Chloroaniline with O,O′-Diphenylphosphorylisothiocyanate. *New J. Chem.* **2016**, *40*, 1230–1236. DOI: 10.1039/C5NJ02588E.

[16] Babashkina, M. G.; Safin, D. A.; Robeyns, K.; Garcia, Y. A Neutral 1D Coordination Polymer Constructed from the Ni^{II} Complex of the *N*-Phosphorylated Thiourea $PhNHC(S)NHP(O)(OPh)_2$ and Pyrazine: A Single-Source Precursor for Nickel Nanoparticles. *Eur. J. Inorg. Chem.* **2015**, *2015*, 1160–1166. DOI: 10.1002/ejic.201402278.

[17] Safin, D. A.; Babashkina, M. G.; Robeyns, K.; Mitoraj, M. P.; Kubisiak, P.; Brela, M.; Garcia, Y. Experimental and Theoretical Investigations of the Ni^{II} Complex with *N*-Phosphorylated Thiourea $iPrNHC(S)NHP(O)(OPh)_2$. *CrystEngComm.* **2013**, *15*, 7845–7851. DOI: 10.1039/c3ce41195h.

[18] Safin, D. A.; Sokolov, F. D.; Szyrwiel, Ł.; Babashkina, M. G.; Gimadiev, T. R.; Hahn, F. E.; Kozlowski, H.; Krivolapov, D. B.; Litvinov, I. A. Nickel(II) Complexes with *N*-(Thio)Phosphoryl-Thioureas $AdNHC(S)NHP(X)(OiPr)_2$: Versatile Coordination of Phosphoryl (X = O) and Thiophosphoryl (X = S) Derivatives. *Polyhedron* **2008**, *27*, 2271–2276. DOI: 10.1016/j.poly.2008.04.014.

[19] Safin, D. A.; Babashkina, M. G.; Bolte, M.; Klein, A. Synthesis and Characterization of *N*-Phosphorylated Thioureas $RNHC(S)NHP(O)(OiPr)_2$ (R = 2-MeC_6H_4, 2,6-$Me_2C_6H_3$, 2,4,6-$Me_3C_6H_2$). *J. Chem. Sci.* **2010**, *122*, 409–413. DOI: 10.1007/s12039-010-0046-3.

[20] Babashkina, M. G.; Safin, D. A.; Bolte, M.; Klein, A. Synthesis of *N*-(Thio)Phosphorylated Thiosemicarbazides $RC(S)NHP(X)(OiPr)_2$ (X = S, R = $NH_2N(Me)$–; X = O, R = $NH_2N(Me)$–, PhNHNH–): Reaction of $NH_2N(Me)C(S)NHP(S)(OiPr)_2$ with Acetone. *Polyhedron* **2009**, *28*, 2693–2697. DOI: 10.1016/j.poly.2009.05.042.

[21] Safin, D. A.; Babashkina, M. G.; Bolte, M.; Klein, A. Synthesis, Characterization and Complexation Properties of *N*-Phosphorylated Thioureas RNHC(S)NHP(O)(O*i*Pr)$_2$ (R = 2-Py, 3-Py) towards Ni(II). *Inorg. Chim. Acta* **2010**, *363*, 1791–1795. DOI: 10.1016/j.ica.2010.02.029.

[22] Safin, D. A.; Babashkina, M. G.; Klein, A.; Sokolov, F. D.; Baranov, S. V.; Pape, T.; Hahn, F. E.; Krivolapov, D. B. The Influence of an Intramolecular Hydrogen Bond on the 1,3-*N*,*S*-Coordination of Crown Ether-Containing *N*-Phosphorylthiourea with Ni^{II}. *New J. Chem.* **2009**, *33*, 2443–2448. DOI: 10.1039/b9nj00252a.

[23] Safin, D. A.; Babashkina, M. G.; Bolte, M.; Klein, A. The Influence of the Spacer Z on *N*-Phosphorylated Bis-Thioureas and 2,5-Dithiobiurea Z[C(S)NHP(O)(O*i*Pr)$_2$]$_2$ (Z = –NHCH$_2$CH$_2$NH–, –NHC$_6$H$_4$-2-NH–, –NHNH–) Crystal Design. *Polyhedron* **2009**, *28*, 1403–1408. DOI: 10.1016/j.poly.2009.02.044.

[24] Camerman, N.; Camerman, A. Cyclophosphamide Structure. Molecular Structure of 4-Ketocyclophosphamide. *J. Am. Chem. Soc.* **1973**, *95*, 5038–5041. DOI: 10.1021/ja00796a042.

[25] *Spartan 14*; Wavefunction, Inc.: Irvine, CA, **2013**.

[26] Frisch, M. J. *GAUSSIAN09*; Gaussian Inc.: Wallingford, CT, **2009**.

[27] Spackman, M. A.; Jayatilaka, D. Hirshfeld Surface Analysis. *CrystEngComm.* **2009**, *11*, 19–32. DOI: 10.1039/B818330A.

[28] Spackman, M. A.; McKinnon, J. J. Fingerprinting Intermolecular Interactions in Molecular Crystals. *CrystEngComm.* **2002**, *4*, 378–392. DOI: 10.1039/B203191B.

[29] Turner, M. J.; McKinnon, J. J.; Wolff, S. K.; Grimwood, D. J.; Spackman, P. R.; Jayatilaka, D.; Spackman, M. A. *CrystalExplorer*; University of Western Australia: Perth, Western Australia, **2017**.

[30] Jelsch, C.; Ejsmont, K.; Huder, L. The Enrichment Ratio of Atomic Contacts in Crystals, an Indicator Derived from the Hirshfeld Surface Analysis. *IUCrJ* **2014**, *1*, 119–128. DOI: 10.1107/S2052252514003327.

[31] Potrzebowski, M. J.; Michalska, M.; Kozioł, A. E.; Kaźmierski, S.; Lis, T.; Pluskowski, J.; Ciesielski, W. Structural Implications of C – H···S Contacts in Organophosphorus Compounds. Studies of 1,6-Anhydro-2-*O*-Tosyl-4-*S*-(5,5-Dimethyl-2-Thioxa-1,3,2-Dioxaphosphorinan-2-Yl)-β-D-Glucopyranose by X-Ray and Solid-State NMR Methods. *J. Org. Chem.* **1998**, *63*, 4209–4217. DOI: 10.1021/jo971294i.

[32] Thomas, S. P.; Spackman, P. R.; Jayatilaka, D.; Spackman, M. A. Accurate Lattice Energies for Molecular Crystals from Experimental Crystal Structures. *J. Chem. Theory Comput.* **2018**, *14*, 1614–1623. DOI: 10.1021/acs.jctc.7b01200.

[33] Mackenzie, C. F.; Spackman, P. R.; Jayatilaka, D.; Spackman, M. A. *CrystalExplorer* Model Energies and Energy Frameworks: Extension to Metal Coordination Compounds, Organic Salts, Solvates and Open-Shell Systems. *IUCrJ* **2017**, *4*, 575–587. DOI: 10.1107/S205225251700848X.

[34] Bader, R. F. W. *Atoms in Molecules: A Quantum Theory; International Series of Monographs on Chemistry*; Oxford University Press: Oxford, UK; New York, 1994.

[35] Lu, T.; Chen, F. Multiwfn: A Multifunctional Wavefunction Analyzer. *J. Comput. Chem.* **2012**, *33*, 580–592. DOI: 10.1002/jcc.22885.

[36] Espinosa, E.; Molins, E.; Lecomte, C. Hydrogen Bond Strengths Revealed by Topological Analyses of Experimentally Observed Electron Densities. *Chem. Phys. Lett.* **1998**, *285*, 170–173. DOI: 10.1016/S0009-2614(98)00036-0.

[37] Cooper, R. I.; Thompson, A. L.; Watkin, D. J. CRYSTALS Enhancements: Dealing with Hydrogen Atoms in Refinement. *J. Appl. Crystallogr.* **2010**, *43*, 1100–1107. DOI: 10.1107/S0021889810025598.

[38] Rigaku, O. D. *CrysAlis PRO*; Rigaku Oxford Diffraction Ltd.: Oxfordshire, UK, **2017**.